MODELING TRANSPORT OF BROMIDE IN FURROW-IRRIGATED FIELD

By Behzad Izadi,[1] Bradley King,[2] Dale Westermann,[3] and Ian McCann[4]

ABSTRACT: The purpose of this study was to investigate the reliability of combining a surface irrigation model (SRFR) and two functional solute transport models (RAO and TETrans) in predicting the position of bromide (Br^-) measured in a 0.81-ha field under furrow irrigation. The SRFR model was used to first predict the infiltrated depths and then RAO and TETrans models were used to predict the position of the solute. Solute was transported according to piston flow theory for the first irrigation and both models predicted the position of the solute with good accuracy. The solute was transported slightly faster than estimated by piston flow for the second irrigation, resulting in a reduction of correct predictions by both models. Both models predicted poorly for the third irrigation because deviations from piston flow were large. RAO model was more successful in predicting the peak solute position, while TETrans was more accurate in predicting mean solute depths. The latter was attributed to the differences between the two models and the sensitivity of TETrans to nodal spacing when predicting peak solute position.

INTRODUCTION

Quantity and chemical quality of water resources are a major concern for heavily irrigated agricultural states. Currently, those involved in irrigation and water management are facing a challenge to conserve water while increasing crop production and avoiding contamination of water supplied. The potential for contamination of ground water by irrigated agriculture is greatest with surface irrigation systems because of possible leaching of fertilizers and pesticides near the inflow end of the field, where excess water application is common. The evaluation of surface irrigation systems requires a knowledge of open channel hydraulics as well as contaminant transport through the vadose zone.

The development of surface irrigation models, [kinematic wave (Walker and Humpherys 1983); zero inertia (Wallender and Rayej 1985; Strelkoff 1990); and full hydrodynamic (Souza 1981; Haie 1983)] enable researchers to simulate entire irrigation events. These numerical models are based on the Saint Venant equations and can be used to predict the quantity and distribution of water applied to the field. However, surface irrigation models are very sensitive to the infiltration function described by the user. Inaccurate description of the infiltration function results in erroneous simulation results (Izadi et al. 1988).

The U.S. Water Conservation Laboratory developed a surface irrigation model (SRFR) (Strelkoff, personal communication, 1990), which simulates flow in furrows, basins, and borders. SRFR is capable of modeling variable conditions (i.e. infiltration and roughness) both in space and time. Furthermore, the user has the option to select between kinematic wave, zero inertia and full hydrodynamic solutions. Version 20.5 of SRFR is user friendly and contains run-time screen graphics (Strelkoff, personal communication, 1993).

Surface irrigation models are not capable of predicting the quality of percolating water due to the lack of a contaminant transport component. Previous attempts to combine a surface model with a mechanistic subsurface model have not been promising due to two major problems (Eddebbarh 1988). First, a physically-based subsurface model requires a large amount of computer memory, and combining the two models requires substantial computer time. Second, it is difficult to gather accurate input parameters and data for field validation of the subsurface model.

An alternative to mechanistic subsurface models are management-oriented models that require fewer input parameters and less computer time. These models are usually based on capacity parameters and are referred to by the term functional (Addiscott and Wagenet 1985). The simplest functional model is based on the piston flow theory, which is the uniform displacement of one solution by another solution from the soil pores, similar to a piston displacing a fluid from a cylinder. The depth of the penetration of the uniform front can be determined by dividing the quantity of the displacing solution by the volumetric water content. Note that piston flow is based on the assumption that incoming and resident solutes do not mix, and it only determines the position of solute front but not its spread.

The management-oriented models may not be less accurate in describing temporally and spatially varied field processes than physically-based models (Wagenet and Rao 1985). Besides the variable field conditions, solute transport may be further complicated by the occurrence of bypass flow. Bypass flow (preferential flow) is here defined as any flow mechanism that causes faster solute movement than that estimated by Darcy flow; for example, flow through macropores.

The management-oriented solute transport models used in this study were the model developed by Rao et al. (1976), hereafter referred to as RAO, and TETrans (Corwin et al. 1991). RAO was selected because it is a simple functional model based on piston flow theory requiring only a small number of inputs, and is field validated (Rao et al. 1976). RAO is capable of predicting solute position but not concentration. In contrast, TETrans is a more complicated functional model which requires more input data and is capable of predicting solute concentration. TETrans was validated using 3 y of lysimeter data (Corwin et al. 1991, 1992).

Izadi et al. (1993) applied a narrow pulse of bromide (Br^-) in a 0.81-ha field and monitored the field scale movement of solute after 3 furrow irrigations. Based on the detection of solute at the furrow shoulders near the edge of the furrows and assumption of one-dimensional solute transport, they concluded that the transport of bromide (Br^-) agreed with piston flow theory for the first irrigation. Piston flow theory also described the position of the Br^- with reasonable accuracy for the second irrigation, but solute was transported slightly faster than predicted by piston flow. However, for the third irrigation which lasted 36 h, piston flow under-predicted the position of the Br^-. It was hypothesized that during the third irrigation, preferential flow occurred after the soil became extremely wet

[1]Assoc. Prof., Bio. and Agric. Engrg. Dept., Moscow, ID 83844-0904.
[2]Asst. Prof., Bio. and Agric. Engrg. Dept., Aberdeen, ID 83210-0530.
[3]Soil Sci., USDA, ARS 3793 North 3600 East, Kimberly, ID 83341.
[4]Assoc. Prof., Dept. of Agric. Mech., Sultan Qaboos Univ., Oman.

Note. Discussion open until September 1, 1996. To extend the closing date one month, a written request must be filed with the ASCE Manager of Journals. The manuscript for this paper was submitted for review and possible publication on December 30, 1993. This paper is part of the ***Journal of Irrigation and Drainage Engineering***, Vol. 122, No. 2, March/April, 1996. ©ASCE, ISSN 0733-9437/96/0002-0090–0096/$4.00 + $.50 per page. Paper No. 7610.

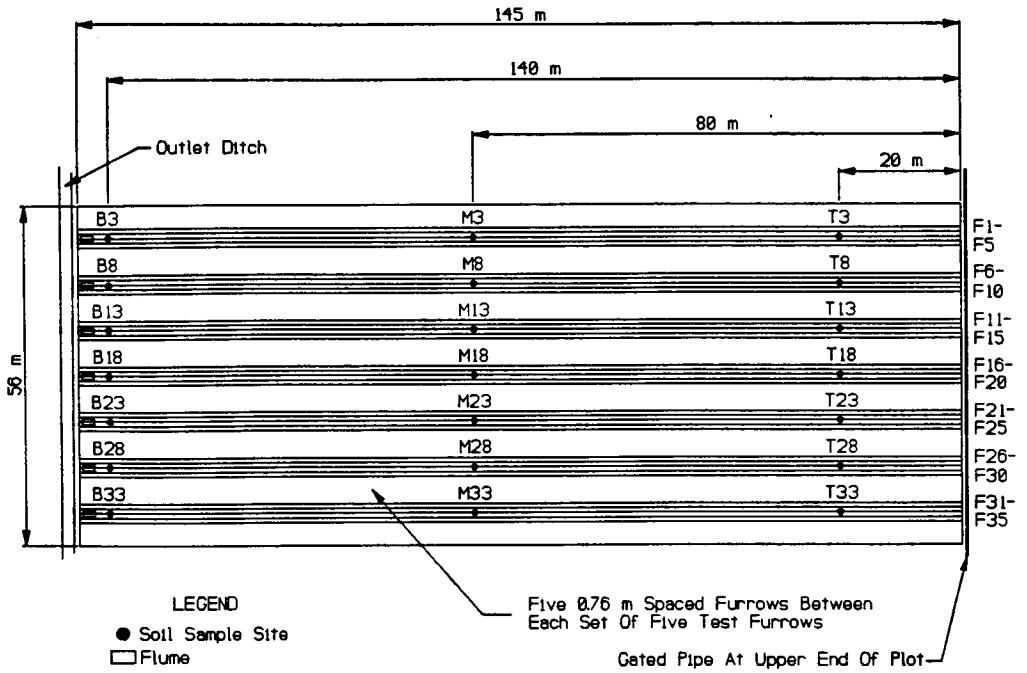

FIG. 1. Plan View of Field Study

and infiltration rates suddenly increased. These results verified studies conducted by Trout and Johnson (1989) on the same soil. They concluded that during long furrow irrigation events, earthworms pierced the wetted perimeter of some furrows, thereby connecting the macropores to the soil surface and increasing furrow infiltration rates.

The objective of the present study was to investigate the reliability of combining SRFR and simple subsurface solute transport models to predict transport of bromide (Br^-) in a furrow irrigated field. Data from the Br^- transport experiment reported above (Izadi et al. 1993) were used.

MATERIALS AND METHODS

Field and Measurements

A Br^- transport study was conducted at the University of Idaho Research and Extension Center during the summer of 1991 in a Portneuf silt loam soil. The details of the experiment can be found in Izadi et al. (1993); however, a brief description of the part of the experiment relevant to this study is given in the following.

Furrows 145 m in length and 0.76 m in spacing were selected in a 0.81-ha fallow field for the Br^- transport study. Three stations located at 20, 80, and 140 m from the furrow inlet were established in each of seven furrows (F3, F8, F13, F18, F23, F28, and F33; Fig. 1). The stations are labeled by the furrow number followed by the letter *T* (top), *M* (middle) or *B* (bottom) indicating its position along the furrow. Two guard furrows were used on both sides of each of the seven monitored furrows, resulting in irrigation of 35 furrows. A narrow pulse of Br^- tracer was applied through a solid-set sprinkler irrigation system and was subsequently transported downward by 26 mm of sprinkler irrigation. Three furrow irrigations were applied at three week intervals during the 63 d study period. Advance and recession data were collected at 20 m intervals during each irrigation. The inflows, advance times, and depth of water infiltrated are shown in Table 1. The inflows and outflows were measured using the bucket and stopwatch method and flumes, respectively. The duration of the first and second irrigations were 8 h, while the third irrigation lasted 36 h. A profilometer (a device for measuring furrow cross-section) was used to determine furrow shape before and after each irrigation. Furrow profile results showed that the wetted perimeters were approximately 8 times smaller than furrow spacing. Soil samples were collected at each station in 0.15 m increments to a depth of 2.4 m prior to each irrigation and at the end of the study period to determine Br^- concentration profile at each station.

Infiltration Function

The infiltration functions were estimated by treating the entire furrow as a infiltrometer.The volume balance method was used to determine the volume of water infiltrated into each furrow after the advance phase was completed

$$V_{inf}(t + \Delta t) = V_{inf}(t) + V_{in}(\Delta t) - V_{out}(\Delta t) - \Delta V_{st}(\Delta t) \quad (1)$$

where $V_{inf}(t + \Delta t)$ = cumulative volume infiltrated at elapsed time $t + \Delta t$, $[L^3]$; $V_{in}(\Delta t)$ = inflow volume during Δt, $[L^3]$; $V_{out}(\Delta t)$ = outflow volume during Δt, $[L^3]$; and $\Delta V_{st}(\Delta t)$ = change in volume of surface storage during Δt, $[L^3]$.

The inflow and outflow volumes were determined from the measurements taken in the field. The average surface flow area was determined by arithmetically averaging the measured inflow and outflow cross-sectional flow areas. This method was not reliable prior to the establishment of the outflow, since the small outflow area resulted in significant underestimation of the average flow area. To circumvent this problem, Elliot and Walker's approach (1982), which estimated the average cross-sectional area of surface flow by multiplying the inlet surface flow area by 0.77, was used early on during the infiltration process. The average depth of infiltration was determined by dividing the final volume infiltrated by the 0.76 m furrow spacing and the 145 m length (Table 1). The variability in infiltration depths was not due to inflow variability, as shown by the low coefficients of variation (CV) for the inflow rates (Table 1). The infiltration variability was greatest for the third irrigation as indicated by the CV value of 28%.

Fitting a proper infiltration equation to the cumulative infiltration data results in an infiltration function that represents the entire furrow. Prior to the curve fitting procedure, the infiltration data were expressed in terms of weighted average furrow opportunity time rather than the elapsed time. The fur-

TABLE 1. Average Inflow Rates, Advance Time to End of Furrow, and Average Depths of Infiltration for Three Irrigations

Furrow Number (1)	Irrigation 1			Irrigation 2			Irrigation 3		
	Q (L min^{-1}) (2)	tad_L* (min) (3)	Z (mm) (4)	Q (L min^{-1}) (5)	tad_L (min) (6)	Z (mm) (7)	Q (L min^{-1}) (8)	tad_L (min) (9)	Z (mm) (10)
3	17	68	42	16	225	59	20	155	294
8	15	80	42	16	303	53	20	156	218
13	16	147	47	15	358	57	19	145	226
18	16	72	45	15	168	53	20	86	116
23	14	122	50	16	164	61	22	137	359
28	16	38	30	16	127	46	21	90	163
33	16	115	46	16	125	44	19	91	166
[Mean]	16	92	43	16	210	53	20	123	227
[CV(%)]	4	38	14	2	40	11	5	24	28

*Time to advance to the end of the field.

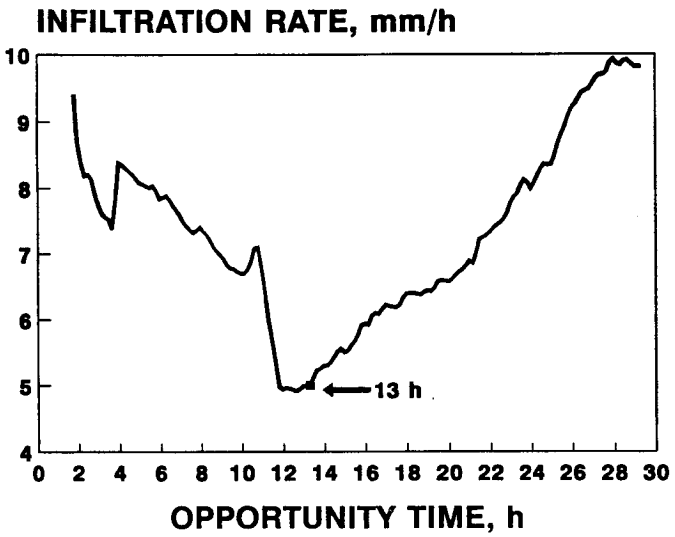

FIG. 2. Infiltration Rate for F3 during Third Irrigation

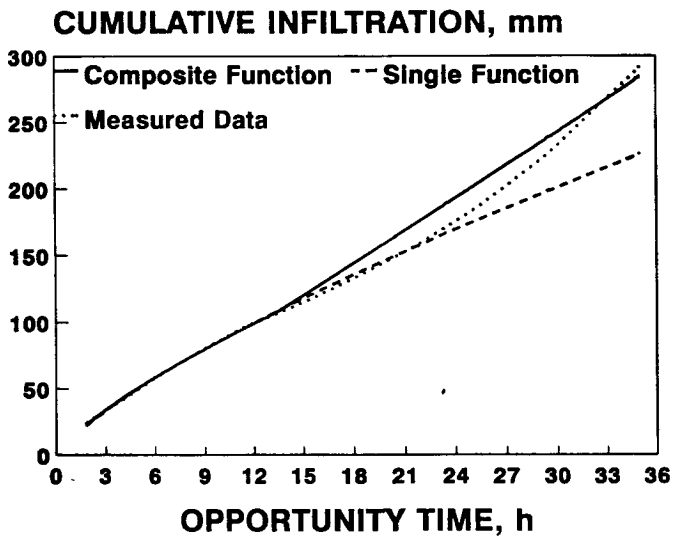

FIG. 3. Measured and Predicted Cumulative Infiltration for F3 during Third Irrigation

row opportunity time is defined as the time for which water is available on the entire furrow for infiltration. The opportunity times for any two locations along the furrow are different, since the advance times to these locations are not the same. Therefore, an equation based on advance data is used to estimate a weighted average value for the furrow opportunity time

$$\tau(t) = \sum_{i=1}^{N} (t - tad_i) \frac{L_i}{L} \tag{2}$$

where $\tau(t)$ = opportunity time at elapsed time t, $[T]$; tad_i = advance time to the ith section, $[T]$; L_i = length of the ith section, $[L]$; L = length of the furrow $[L]$; and N = number of furrow sections.

Eight sections were used to calculate $\tau(t)$ in (2). Preliminary investigation of the cumulative infiltration data indicated that the Kostiakov function was an appropriate infiltration equation

$$Z = k\tau^a \tag{3}$$

where Z = cumulative infiltrated depth, $[L]$; k = Kostiakov coefficient, $[LT^{-a}]$; and a = Kostiakov exponent. In most cases an R^2 greater than 0.99 resulted from the curves fitted to the data.

The cumulative infiltration data for the third irrigation indicated an increase in infiltration rate, 6 to 13 h after the start of the irrigation, for all seven furrows. This unusual infiltration trend was also reported by Trout and Johnson (1989) for the same soil and is depicted in Fig. 2 for F3. Although fluctuations in infiltration rate might be related to the changes in inflow rate or the possibility of measurement errors, it is evident that the infiltration rate continuously increased after 13 h. Accordingly, the infiltration was described by two different infiltration functions. The time τ_1, at which the infiltration rate began to increase was determined for the infiltration rate curves. For example for F3, τ_1 occurred after 13 h (Fig. 2). Two Kostiakov functions were then fitted to the cumulative infiltration data corresponding to $\tau \leq \tau_1$ and $\tau > \tau_1$. The composite function better estimated the final infiltrated depth than a single Kostiakov function as depicted for F3 in Fig. 3.

In irrigation management studies, estimation of the furrow infiltration function is often desired early in the irrigation. Accordingly, furrow infiltration functions were also estimated using only the first half of the collected data (50% of the original opportunity times), and a single Kostiakov function. Furrow infiltration functions were also estimated during the advance phase according to the two-point method (Elliot and Walker 1982). However, both methods significantly underestimated the volume infiltrated during the third irrigation. Due to the significance of the third irrigation in the transport of bromide, these methods were not considered further in the present study.

SRFR Model

SRFR [version 20.5 (Strelkoff, personal communication, 1993)] was used to simulate the furrow irrigation events and predict the infiltrated depth at each station. A sample input data set is presented in Tables 2 and 3. The parameter τ_1 indicates the time at which the infiltration function was changed.

TABLE 2. Input Data to SRFR Model for Simulating Third Irrigation of F3

Input data (1)	Variable (2)	Unit of measurement (3)	Value (4)
Furrow length	L	m	145
Inundation-time segment, τ_1	τ_1	h	13
Kostiakov k parameter	$t \leq \tau_1$	mm h^{-a}	15.61
Kostiakov a parameter	$t \leq \tau_1$	—	0.748
Kostiakov k parameter	$t > \tau_1$	mm h^{-a}	6.24
Kostiakov a parameter	$t > \tau_1$	—	1.065
Manning's roughness	n	—	0.04
Slope	S_0	mm^{-1}	0.0125
Coefficient[a]	C_1	mm^{1-c2}	11.36
Exponent[a]	C_2	—	0.772
Furrow spacing	SP	m	0.762

[a]In a power function describing top width (TW) of the furrow, TW = $C_1 y^{c2}$, where y = depth of flow.

TABLE 3. Input Inflow Hydrograph Data to SRFR Model for Simulating Third Irrigation of F3

Time (Min) (1)	Inflow ($1\ s^{-1}$) (2)
0	0.329
30	0.329
290	0.294
670	0.291
690	0.329
1,455	0.341
1,810	0.344
1,815	0.421
2,137	0.379
2,151	0.379
2,152	0

Note that shifting from the first infiltration function to the second will result in a discontinuity in cumulative infiltration. However, the model automatically adjusts the cumulative infiltration by adding a constant storage term to the second infiltration function to maintain a smooth transition between the two functions as shown by the composite curve in Fig. 3. Due to the relatively steep furrow slope (1.25%), the kinematic wave option of SRFR was used. The output for each furrow irrigation simulation included the infiltration depth at different locations along the furrow. This output was used to estimate, by interpolation, the amount of infiltration at distances of 20, 80, and 140 m, corresponding to the 3 stations in each monitored furrow.

TETrans Model

TETrans is a functional model which predicts solute concentration for each soil compartment based on solute mass balance. In TETrans the soil is divided into a maximum of 25 compartments and the net water input is transported downwards after increasing the water content to field capacity. Therefore, it is an event-based model which does not consider lag times. After an irrigation event, the total solute mass in a given soil compartment is estimated based on one of three possible situations, depending on the amount of water entering the soil compartment (V_{in}), the resident soil water content and the field capacity value. First, if V_{in} is large enough to displace all the resident soil water and bring the water content to field capacity then $V_{in} > V_{fc}$

$$V_{AI} = V_{fc}; \quad T_{AI} = V_{fc} C_{in} \tag{4a,b}$$

where V_{fc} = volume of water in soil compartment after it has reached field capacity [L^3]; V_{AI} = volume of water in soil compartment after an irrigation [L^3]; C_{in} = solute concentration of water entering soil compartment [ML^{-3}]; and T_{AI} = total amount of solute in soil compartment after irrigation [M].

Second, if V_{in} is not enough to displace all the resident solid water but large enough to bring the water content to field capacity then $V_{fc} - V_{BI} < V_{in} < V_{fc}$

$$V_{AI} = V_{fc} \tag{5a}$$

$$T_{AI} = (V_{fc} - V_{in}) C_{BI} + V_{in} C_{in} \tag{5b}$$

where V_{BI} = volume of water in soil compartment immediately before irrigation [L^3]; and C_{BI} = solute concentration in soil compartment immediately before irrigation [ML^{-3}].

Third, if V_{in} is not enough to bring the water content to field capacity then $V_{in} < V_{fc} - V_{BI}$

$$V_{AI} = V_{in} + V_{BI} \tag{6}$$

$$T_{AI} = V_{BI} C_{BI} + V_{in} C_{in} \tag{7}$$

The inputs to TETrans are the amount of irrigation, precipitation, and evaporation for each date, and solute concentration in the input water. For each soil compartment, field capacity, minimum water content, bulk density, resident solute concentration, initial water content, and compartment thickness must be specified.

RAO Model

RAO is a model based on piston flow which predicts the position of the solute (d_s). The inputs to the model are as follows: time increment D_t, depth increment D_z, initial water content (θ_i), water content at field capacity (θ_{fc}), days to reach field capacity after each irrigation event, daily irrigation, precipitation, and bare soil evaporation. It is assumed that the water evaporated from the surface is extracted from the top 0.3 m of the soil, with 60% of the extraction occurring from the top 0.15 m depth. For a given irrigation event, the effective irrigation depth (I_e) is defined as the net depth of irrigation water in excess of the amount needed to fill the profile above the solute position, $d_s(t)$, to field capacity. The solute is moved downwards according to the effective irrigation depth

$$d_s(t + D_t) = d_s(t) + I_e/\theta_{fc} \tag{8}$$

Model Sensitivity

A sensitivity analysis was performed to compare the predictions of the two models and determine the effect of important input parameters on the simulated outputs. It was assumed that a soil column with a nodal spacing of 0.15 m, an initial volumetric water content of 0.20 and field capacity of 0.31, was irrigated with 75 mm of water after application of a narrow pulse of solute. RAO and TETrans simulations were performed by varying an input parameter (field capacity, irrigation amount, initial water content, and nodal spacing) by 30% while keeping the rest of the inputs constant and predicting the position of solute (RAO's output) or the soil concentration profile (TETrans' output). In the latter case, the depth of maximum concentration (MODE) and the mean depth of solute transport (MEAN) were determined from each simulated soil concentration profile

$$\bar{z} = \frac{\sum_{i=1}^{N} z_i M_i}{\sum_{i=1}^{N} M_i} \tag{9}$$

where $\bar{z}$ = mean depth of solute transport [L]; z_i = distance from soil surface to middle of ith soil compartment [L]; M_i =

TABLE 4. Results of Sensitivity Analysis Performed on RAO and TETrans Models[a]

fc[b] (1)	I[c] mm (2)	θ_i (3)	D_z m (4)	TETrans MODE m (5)	TETrans MEAN m (6)	RAO d_s m (7)
0.31	75	0.20	0.15	0.225	0.26	0.17
0.403	75	0.20	0.15	0.225 (0)	0.23 (12)	0.13 (24)
0.217	75	0.20	0.15	0.225 (0)	0.41 (58)	0.24 (41)
0.31	97.5	0.20	0.15	0.225 (0)	0.32 (23)	0.24 (41)
0.31	52.5	0.20	0.15	0.225 (0)	0.23 (12)	0.09 (47)
0.31	75	0.26	0.15	0.225 (0)	0.29 (12)	0.17 (0)
0.31	75	0.14	0.15	0.225 (0)	0.24 (8)	0.17 (0)
0.31	75	0.20	0.20	0.300 (33)	0.30 (15)	0.17 (0)
0.31	75	0.20	0.10	0.150 (33)	0.24 (8)	0.17 (0)

[a]The first row is the standard simulation and the numbers in the parentheses denote percent deviations from the results of the standard simulation.
[b]Field capacity.
[c]Irrigation amount.

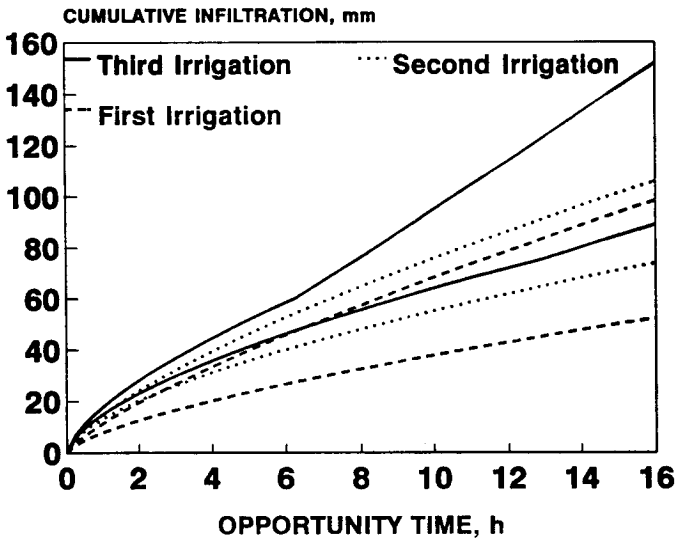

FIG. 4. Lowest and Highest Infiltration Functions Predicted for Each Irrigation

amount of solute mass recovered from ith soil compartment [M]; and N = number of soil compartments.

The results of the sensitivity analysis are shown in Table 4. The predicted MODE was not affected by changes in field capacity, irrigation amount and initial water content, while it was significantly affected by the changes in nodal spacing. The predicted MEAN and d_s were equally affected by changes in field capacity, while predicted d_s was more sensitive to changes in the irrigation amount. Changes in initial water content did not affect RAO's predictions, since solute movement was only dependent on the net water input and field capacity according to (8). In contrast, MEANs predicted by TETrans were mildly affected by changes in water content. Whenever the solute front lied within a compartment, the initial water content was used to estimate the amount of solute within that compartment according to (7). Note that V_{BI} in (6) and (7) was a function of the initial water content. The changes in the initial water content did not significantly affect MEAN predictions, since (7) was only used for one compartment that contained the solute front. RAO's predictions were not affected by changes in nodal spacing, since the principal equation (8) was independent of D_z. MEANs predicted by TETrans were mildly affected by changes in nodal spacing since, by altering D_z, the thickness of the compartment that contained the solute front was changed and the effect of initial water content in estimating solute amount (7) was modified.

Model Inputs

A nodal spacing of 0.15 m was selected, since the measurements for bulk density, initial water content, and solute content were also taken every 0.15 m. Preliminary TETrans simulations indicated that selection of finer nodal spacing would result in erroneous MEAN estimations, since due to short column length appreciable amount of solutes would leach out of the column. Selection of the maximum 25 compartments with a uniform thickness of 0.15 m resulted in a sufficiently long column (3.75 m) to prevent transport of solutes beyond the lower boundary. A value of 0.31 for volumetric field capacity and a duration of 5 days to reach field capacity was selected based on the previous study in this field (Izadi et al. 1993). The narrow pulse of Br^- was considered as a 3.3-mm irrigation on the first day with a concentration of 1,372 mg L^{-1}.

RESULTS AND ANALYSIS

Fig. 4 depicts the lowest and highest infiltration functions for each irrigation. Under normal conditions, the first irrigation is expected to have the highest infiltration variability, since

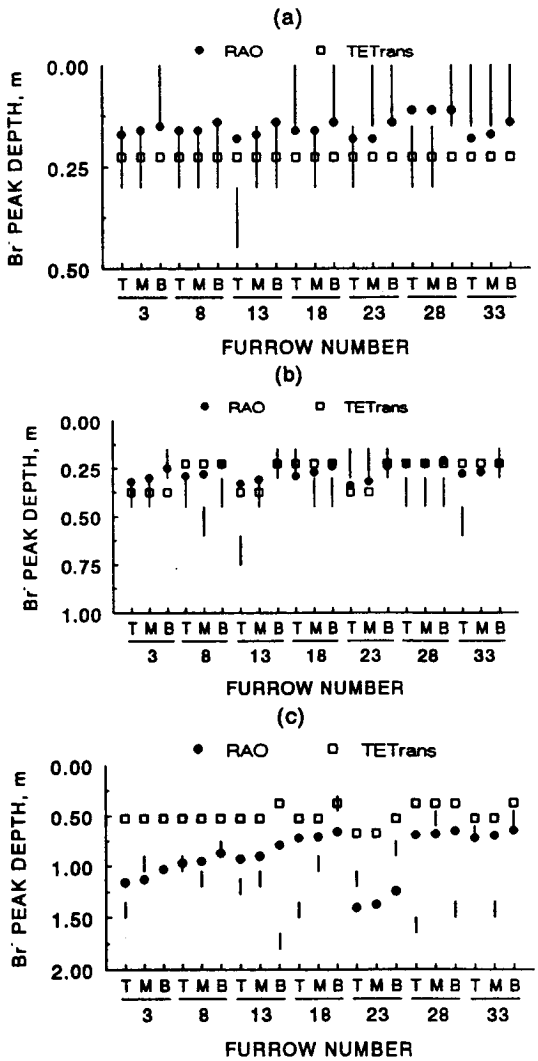

FIG. 5. Measured and Predicted Peak Br^- Position at Each Station for: (a) First Irrigation; (b) Second Irrigation; (c) Third Irrigation (Vertical Bar Represents 0.15 m Depth Increment in which Br^- Peak Was Observed

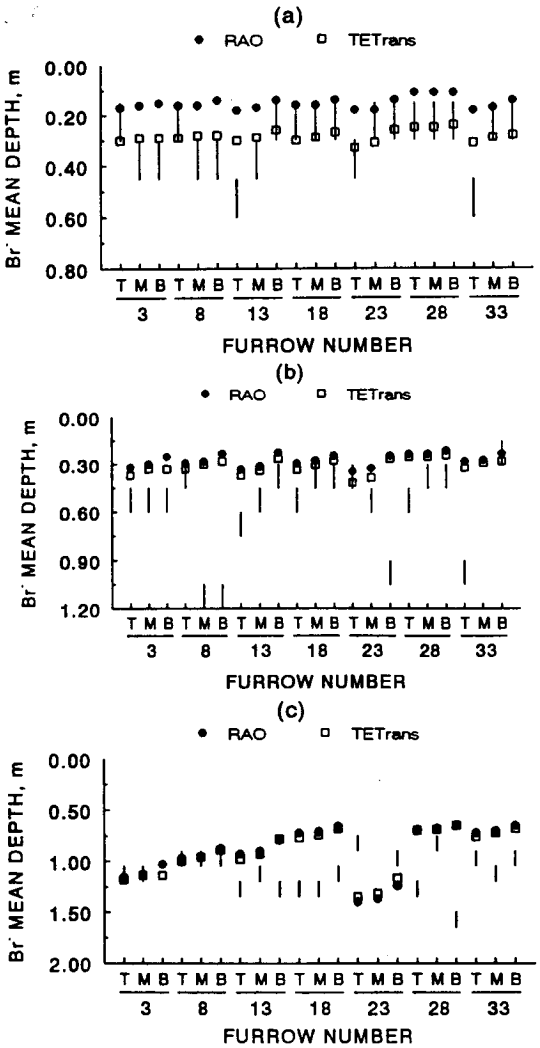

FIG. 6. Measured and Predicted Mean Br^- Depth at Each Station for: (a) First Irrigation; (b) Second Irrigation; (c) Third Irrigation (Vertical Bar Represents 0.15 m Depth Increment in which Br^- Mean Was Measured

furrows may differ in terms of roughness, shape, and compaction. Furrow infiltration variability is expected to decrease later in the irrigation season as the furrow shape and soil conditions become more uniform. It is evident from the infiltration functions that the first and second irrigations followed the normal trend, while the third irrigation results in unusually high infiltration amounts and infiltration variation (Table 1 and Fig. 4).

The infiltration functions were used in SRFR model to simulate each irrigation and predict the amount infiltrated at each station. The simulated infiltration depths were used in RAO and TETrans models to predict the transport of the Br^-. Figs. 5 and 6 depict the predicted and measured MODEs and MEANs, respectively after each irrigation. The vertical bar represents the 0.15-m depth increment in which the Br^- peak or mean was measured. Due to very low Br^- recovery values, the measurements for station 33M in the second irrigation and stations 3B and 23M in the third irrigation are not considered in the analysis. Note that RAO resulted in only one set of predicted values, while TETrans model predicted both the MODEs and MEANs.

For the first irrigation, RAO predicted the correct MODE in 15 of the 21 stations, with predictions for 3 other stations off by only 0.03 m (Fig. 5a). The number of correct predictions by RAO reduced to 9 for the second irrigation with predictions for 4 other stations within 0.02 to 0.04 m of the observed values (Fig. 5b). In the third irrigation, RAO predicted the correct position in only 3 of the 21 stations (Fig. 5c). The same trend was also observed in TETrans simulations, in which the number of correct MODE predictions was 11, 7, and 1 for the first, second, and third irrigation, respectively (Figs. 5a–5c).

Considering the MEAN, RAO predicted the correct position in 14 of 21 stations after the first irrigation, while TETrans simulations resulted in 17 correct predictions with 2 other predictions off only by 0.02 m (Fig. 6a). The number of correct predictions by RAO and TETrans reduced to 3 and 4 for the second irrigation, respectively (Fig. 6b). However, the predictions of TETrans were only off by 0.03 to 0.06 m for 4 additional stations. Both models predicted the MEAN correctly for only 5 stations after the third irrigation (Fig. 6c).

In general, RAO predicted the movement of peak Br^- with better accuracy, while TETrans results were more accurate for the mean predictions. The latter is because TETrans is rather insensitive to nodal spacing when prediction mean values, while the peak predictions are affected by the spacing of the nodes (Table 4). The differences in results between the two models is attributed to the way each model considers the solute transport. TETrans uses a solute mass balance to predict the amount of solute in each compartment given the water content, bulk density, and soil solution concentrations. In contrast, RAO uses a water balance, and estimates the movement of solute according to effective irrigation depth (I_e).

Considering a 0.06 m tolerance, RAO predicted the correct MODEs for 18, 13, and 3 stations, while TETrans' predictions of MEANs were accurate for 19, 8, and 6 stations, respectively for the first, second, and third irrigation. These results can be explained by the way solute was transported during the three irrigations as reported by Izadi et al. (1993). During the first irrigation Br^- was transported according to piston flow theory, and both models predicted the peak and mean depth of the solute with good accuracy. The transport of solutes were slightly faster than those predicted by piston flow for the second irrigation. Consequently, the number of current predictions reduced for both models. The deviations from piston flow were more pronounced for the third irrigation which caused further reduction in the number of correct predictions.

The measured concentration profiles were plotted against the profiles predicted by TETrans for all 21 stations. A comparison of the plots indicates similar conclusions as mentioned above. Typical plots for station 18M are shown in Fig. 7. In the first irrigation, the simulated and measured profiles were similar in shape and magnitude (Fig. 7a); in the second irrigation the simulated profile slightly lagged the measured profile (Fig. 7b); and in the third irrigation the differences between the profiles were considerable (Fig. 7c).

Sources of Error

The differences between measured and predicted solute positions can be attributed to inaccurate estimation of model inputs and the simplicity of the subsurface models. The models were most sensitive to the estimated field capacity and irrigation amount. The field capacity value was estimated with reasonable accuracy based on the water content measurements, and was within the range of values estimated in previous studies at the same site (Wright, personal communication, 1992).

The irrigation depths were predicted by SRFR model using the estimated infiltration functions which were averaged over the furrow length and spacing. However, furrow infiltration is two-dimensional with the greatest infiltration depth expected beneath the furrow bottom and the lowest under the furrow bed. It is possible that the irrigation depths, which were predicted based on average infiltration functions, were not accurate estimates of the infiltration depths at the furrow shoulders, where the soil samples were collected.

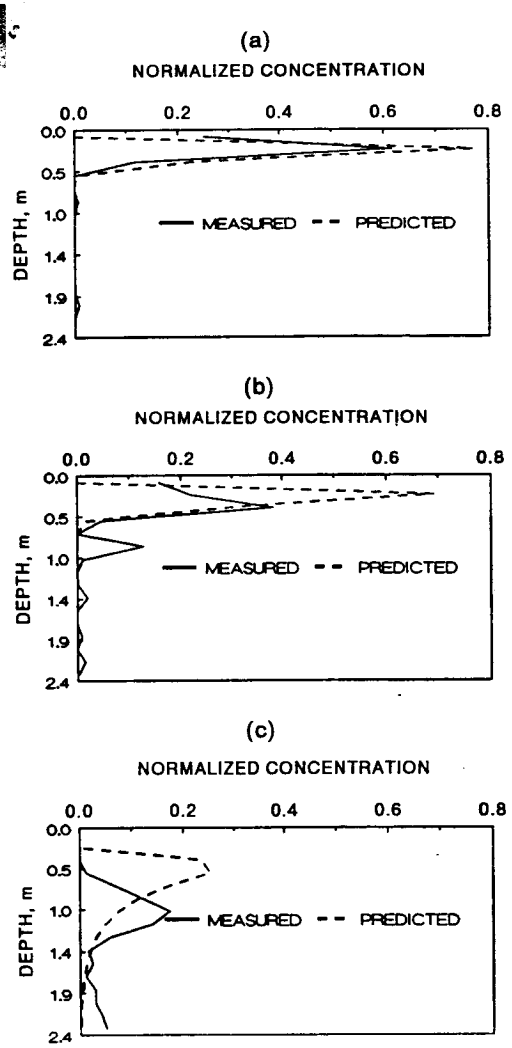

FIG. 7. Measured and Predicted Br^- Profiles at Station 18M for: (a) First Irrigation; (b) Second Irrigation; (c) Third Irrigation

Another source of error in estimating the irrigation depths might have been the spatial variability of the soil infiltration rates. Although each furrow had its unique infiltration function, infiltration variability along each furrow was not considered in the analysis. SRFR model predicted the infiltration depth at the three stations along a furrow according to the corresponding opportunity times using only one infiltration function. In most cases, the opportunity times along each furrow were not significantly different, since the durations of the advance phases were small compared to the total irrigation times. This was particularly true for the third irrigation with the longest irrigation time. Consequently, SRFR model predicted similar irrigation depths at the top, middle, and bottom of each furrow, which resulted in prediction of similar solute depths by the functional models.

CONCLUSIONS

A surface irrigation model (SRFR) and two functional subsurface solute transport models (RAO and TETrans) were used to predict the position of bromide (Br^-) transported by three furrow irrigation events. Solute transport followed piston flow theory for the first irrigation, and both models predicted Br^- position with good accuracy. The solute was transported slightly faster than estimated by piston flow for the second irrigation, resulting in a reduction of correct predictions by both models. The deviations from piston flow were large for the third irrigation resulting in further reduction of correct predictions. The RAO model was more successful in predicting the peak solute position, while TETrans predictions were more accurate in predicting mean solute depths. The latter was attributed to the differences between the two models and the sensitivity of TETrans to nodal spacing when predicting peak solute position. Considering the simplicity of the subsurface models and sources of error, the simulation methodology is appropriate for this type of soil as long as the solute transport does not significantly deviate from the piston flow theory. Further development of this methodology is needed to include the effect of infiltration variability along the furrow and consider the possibility of bypass flow.

Simple one-dimensional models such as those investigated in this study are useful for irrigation and nitrogen management studies, since they require less input parameters that can be easily obtained. However, the nature of furrow infiltration is two-dimensional, and depending on the soil texture, soil hydraulic properties, furrow spacing and mode of fertilizer application a significant portion of the fertilizer might be transported laterally. Therefore, field experiments investigating the two-dimensional solute transport combined with more comprehensive two-dimensional models would be useful for future development of irrigation and nitrogen management practices.

APPENDIX. REFERENCES

Addiscot, T. M., and R. J. Wagenet. (1985). "Concepts of solute leaching in soils: a review of modeling approaches." *Soil Sci. Soc. of Am. J.*, 36, 411–424.

Corwin, D. L., Waggoner, B. L., and Rhoades, J. D. (1991). "A functional model of solute transport that accounts for bypass." *J. Envir. Quality.*, 20(3), 647–658.

Corwin, D. L., Waggoner, B. L. and Rhoades, J. D. (1992). "Simulating the movement of a reactive solute through a soil lysimeter column using a functional transport model." *J. Envir. Sci. Health*, A27(7), 1875–1913.

Eddebbarh, A. (1988). "An integrated surface-subsurface flow model and evaluation of infiltration functions used in surface irrigation." PhD dissertation, Colorado State Univ., Fort Collins, Colo.

Elliott, R. L., and Walker, W. R. (1982). "Field evaluation of furrow infiltration and advance functions." *Trans. of the ASAE*, 15(2), 396–400.

Haie, N. (1983). "Hydrodynamic simulation of continuous and surged surface flow," PhD dissertation, Utah State Univ., Logan, Utah.

Izadi, B., Heermann, D. F., and Duke, H. (1988). "Sensor placement for real time infiltration parameter evaluation." *Trans. of the ASAE*, 13(4), 1159–1166.

Izadi, B., King, B., Westermann, D., and McCann, I. (1993). "Field-scale transport of bromide under variable conditions observed in a furrow irrigated field." *Trans. of the ASAE*, 36(6), 1679–1685.

Rao, P. S. C., Davidson, J. M., and Hammond, L. C. (1976). "Estimation of non-reactive and reactive solute front locations in soils." *Proc., Hazardous Wastes Res. Symp.*, Tucson, Ariz., U.S. Environmental Protection Agency, EPA-600/9-76-015.

Souza, F. (1981). "Nonlinear hydrodynamic model of furrow irrigation," PhD dissertation, Univ. of California, Davis, Calif.

Strelkoff T. (1990). "SRFR, a computer program for simulating flow in surface irrigation." *WCL Rep. No. 17.*, U.S. Water Conservation Lab., Phoenix, Ariz.

Trout, T. J., and Johnson, G. S. (1989). "Earthworms and furrow irrigation infiltration." *Trans. of the ASAE*, 32(5), 1594–1598.

Wagenet, R. J., and Rao, P. S. C. (1985). "Basic concepts of modeling pesticide fate in the crop root zone." *J. Weed Sci.*, 33, 25–32.

Wallender, W. W., and Rayej, M. (1985). "Zero-inertia surge model with wet-dry advance." *Trans. of the ASAE*, 28(5), 1530–1534.

Walker, W. R., and Humpherys, A. S. (1983). "Kinematic wave furrow irrigation model." *J. Irrig. and Drain. Div.*, ASCE, 109(4), 377–392.